ACOUSTIC EMISSION MONITORING OF A WIND TURBINE BLADE DURING A FATIGUE TEST*Ψ

A.G. Beattie
Department 9742
Sandia National Laboratory
Albuquerque, NM 87185

ABSTRACT

A fatigue test of a wind turbine blade was conducted at the National Renewable Energy Laboratory. Acoustic emission monitoring of the test was performed, starting with the second loading level. The acoustic emission data showed that this load exceeded the strength of the blade. An oil can type of deformation was seen in two areas of the upper skin of the blade from the beginning of the second loading. One was near the blade root and the other was at about 35% of the span. The acoustic emission data indicated that no damage was taking place near the root, but in the deforming area at 35% span, damage occurred from the first cycles of the second load. The test was stopped after approximately one day, although no gross damage had occurred. Several weeks later the test was resumed. Gross damage occurred in approximately one half hour. The emission data showed evidence of a possible second damage site.

INTRODUCTION

One of the most common materials used in the construction of large wind turbine blades is fiberglass reinforced plastic (FRP). A number of failures of such blades has shown a need for both static and fatigue testing of new blade designs as well as a better knowledge of the type and magnitude of real wind loads on the blades. The National Renewable Energy Laboratory (NREL) has an ongoing program of static and fatigue load tests on large wind turbine blades. Such testing is expensive and can be very time consuming for fatigue tests. Conventional instrumentation on these tests usually consists of strain gauges. Strain concentrations in fiber glass blades can be quite localized and the number of strain gauges that would be needed to accurately map out the strain fields on a blade would be both expensive and complicated. However a test which only determines the static failure load or the number of fatigue cycles at a given load and frequency to failure, while valuable, is only a small part of the information which could be obtained. Therefore several new methods of instrumentation aimed at acquiring failure information on critical areas of the blade have been tried. These include acoustic emission (AE) and optical and thermal imaging methods[1]. This paper describes the acoustic emission monitoring of a fatigue test on a twenty meter blade.

Acoustic emission testing[2,3] has been used for years to test metallic structures. More recently it has become the primary method of testing FRP tanks and structures. Some of the sources of the emission in FRP are matrix cracking, fracture of the matrix-fiber interface and fracture of the fiber. All are present in the failure of FRP. The two most significant failure mechanisms in a wind turbine blade are cracking in the bond between two pieces of the structure, such as a joint between a spar and the skin, and tears in the skin or a spar. Both involve the progressive fracture of many fibers. AE has been very successful at detecting all of these failure mechanisms and sometimes identifying them from amplitude analysis of the AE signals. However in large structures, the high acoustic attenuation in FRP precludes amplitude analysis unless the origin of the individual signals can be identified and corrections for the distances traveled applied to the signal amplitudes. The usual method of testing FRP structures has been to apply an array of sensors spaced so that a moderate amplitude AE signal occurring midway between them will just barely .trigger each sensor. One then looks at broad areas of damage defined as the area within the range of each individual sensor. Source location based upon times of signal flight to multiple sensors has seldom been tried on large FRP structures. Unfortunately, in testing wind turbine blades, one would like a relatively high location accuracy so that one could determine whether the failure was strictly in the skin or in the skin-spar bond or a spar failure. In a fatigue test, much time could be saved if a region of failure could be identified long before actual failure occurred. Even when the blade is taken to failure, it would be extremely valuable to identify other regions, commonly called secondary failure zones, that showed damage, though of lesser magnitude.

Very little work has been done on AE time of flight

* This work is supported by the U. S. Department of Energy under Contract DE-AC04-94AL85000.

source location or monitoring of fatigue tests of large FRP structures. Wei and McCarty[4] performed fatigue tests on a 7. 5 and a 13 meter wind turbine blade. They monitored the AE during static tests between intervals of at least 10,000 cycles. No monitoring was done during the actual fatigue test and only 4 sensors were used in a linear array on the first 20 inches of the blade root.

Working in conjunction with NREL, we have used AE source location techniques to monitor a static load test of a 9 meter blade. The test successfully detected both the onset and the location of the failure in real time and also detected a bond failure between skin and beam which was verified when the blade was sectioned. The FRP skin of this blade had a large frequency dependent attenuation. However, linear AE location was successfully performed by using low frequency (60 KHz) sensors and relatively short intersensor spacings (760mm). Our first attempt to use AE source location on the surface of a blade during a fatigue test showed that source location was possible but not easy. Every sensor saw a large amount of AE but most of it occurred during the maximum rate of load change (rising and falling), not at the peak load. A laboratory study indicated that major damage to the FRP and the resulting AE occurs at the peak load during the progress of a fatigue test. Therefore, a voltage controlled gate controlled by the load cell signal was used to restrict data acquisition to the time around the peak load. The time gating combined with low frequency sensors and relatively short (760mm) sensor spacings did allow AE source location on the portion of the surface of the blade covered by the sensor array. Full coverage of both surfaces would have required a large number of sensors. Only the critical regions could be covered. With the measured attenuations and 60 KHz sensors, the area per sensor that could be covered using AE source location was between 300 and 600 square inches.

TEST DESCRIPTION

The wind turbine blade in this test was a prototype of a twenty meter blade. The blade was constructed of FRP which was bonded to a steel flange at the root. The blade was mounted horizontally in a flap direction with its root attached to a rigid steel mounting assembly. The outer 35% of the blade was removed to prevent it from hitting the roof of the building. The stub was covered and a hydraulic actuator was attached at the stub end. This actuator was capable of exerting a vertical force of40% about 28,000 lbs., with a maximum displacement of twenty inches. The actuator was operated sinusoidally at 0. 75 Hz giving a maximum of 64,800 cycles per day. All tests were run with a positive load only, extending from 10% of peak load to peak load and back.

The acoustic emission was detected with a Physical Acoustics Corporation (PAC) Spartan AT acoustic emission system. This system has 24 data channels. Every channel can measure and record several parameters for each acoustic emission signal. Parameters collected in this test were the acoustic emission count, the signal length, the signal rise time, the signal peak amplitude and the area under the signal voltage-time curve (signal strength or "energy"). The system measures and records the absolute time of signal arrival at the sensor to within about 0. 25 microseconds and assigns the approximate load at the time of the signal. This load is sampled 100 times per second but assigned to the hit after the data arrives at the main computer. Data pile up can cause the load to be out of synchronization with the signal arrival time. Therefore the "measured" load can be a misleading parameter in this type of test. This system had the capacity to collect a one gigabyte data file on the hard disk before the data had to be transferred to storage. Such a file would hold parameters from over 40 million emission signals

PAC R61 sensors were used in this test. These sensors have an integral 40 dB preamplifier built into them, powered from the main system through the signal cable. The peak sensitivity of the sensors is near 60 KHz with reasonable response to below 30 KHz. The sensors were applied to the blade with GE Silicone II household cement, used as both glue and acoustic couplant. This material is both a good couplant and an excellent glue for fatigue tests.

The first segment of this test consisted of one million cycles at a relatively low peak load. Failure was not anticipated at this load so there was no acoustic monitoring of this segment. The load was then increased by 25%. The blade root region flange was not thought to be a problem because of extra fiberglass reinforcement around the first four feet of the blade. One sensor was placed on this reinforcement to detect any acoustic signals propagating into the blade from the steel mounting assembly, a problem that had been encountered in a previous test.

A brief run at the new load showed that an "oil can" deformation of the upper skin of the blade was taking place in two areas. The acoustic emission sensor array was then designed to cover these two areas as well as the root region just outside of the reinforced region. The complete sensor layout is shown in Figure 1. Sensor 24 was placed 60 inches past the top surface array to detect any acoustic signals traveling down the blade from the actuator.

The root array consisted of two rows of four sensors each, one row offset by 45 degrees from the other, covering the region with eight adjacent triangles. The sensor spacing in a row was 41 inches and the rows were 40 inches apart. Because of the high attenuation, this

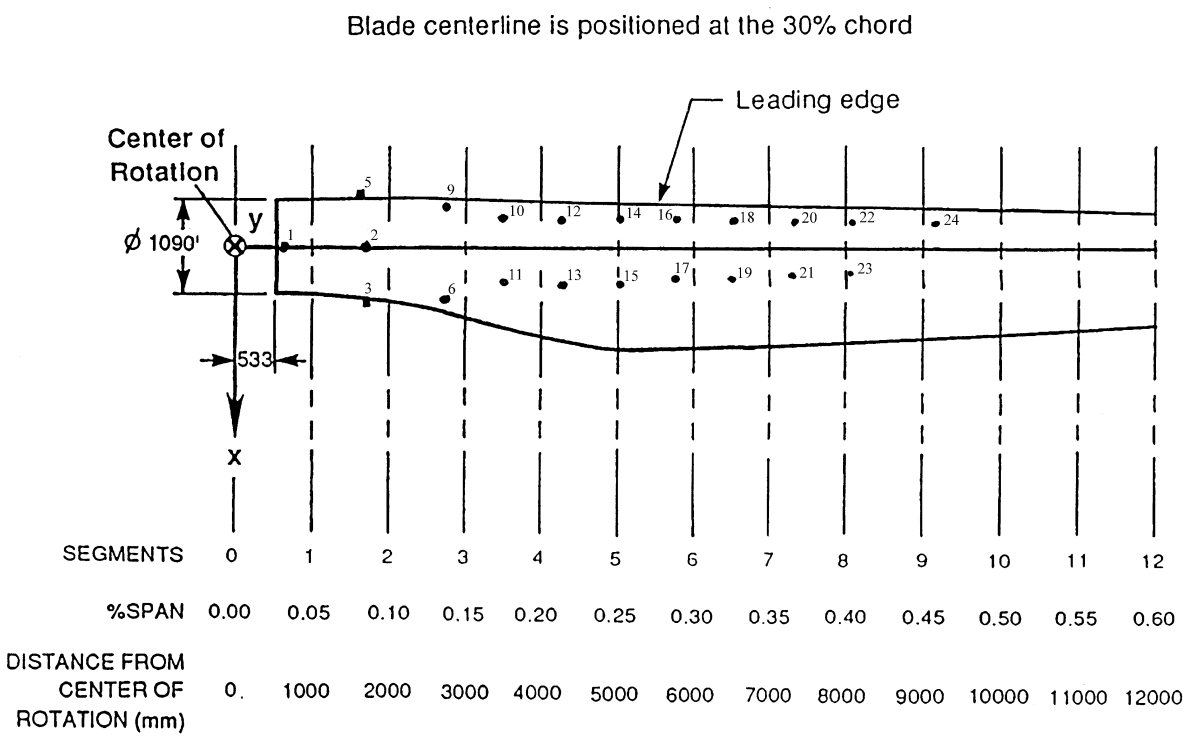

Figure 1. Blade and Sensor Layout

was as far apart as the sensors could be placed with any assurance that moderate amplitude emission sources would be detected at all sensors of a triangle. Ideally, more sensors would have been used on this region but, with only 24 channels available, that would have precluded two-dimensional location in the oil can regions.

The sensor array on the surface of the blade consisted of two rows of seven sensors each, set up to form a pattern of adjoining rectangles. The front row was set approximately on top of the front spar and the second row was set roughly on top of the second spar. Spacing between the sensors in each row was 30 inches with about 30 inches between rows (the two spars were not parallel).

A previous fatigue test of a wind turbine blade had shown that many acoustic signals were detected during a single fatigue cycle. The largest number occurred during the times of the maximum rate of the load change, both on increasing and decreasing loads. These events were thought to be caused, at least in part, by rubbing of non-bonded surfaces in the blade. In any case, they did not arise from fatigue damage in the previous test. For this blade, initial measurements showed a data rate of about 40 megabytes per hour. To reduce the amount of data collected and to keep primarily signals that were produced by fatigue damage, a voltage controlled gate was used with the system. The gate was triggered off the load cell and permitted the system to take data only when the load was above 90% of the maximum load. This procedure reduced the collected data rate to about 10 megabytes per hour. While this is still very large, it did allow the collection of four days' worth of data at this rate before the disk was full.

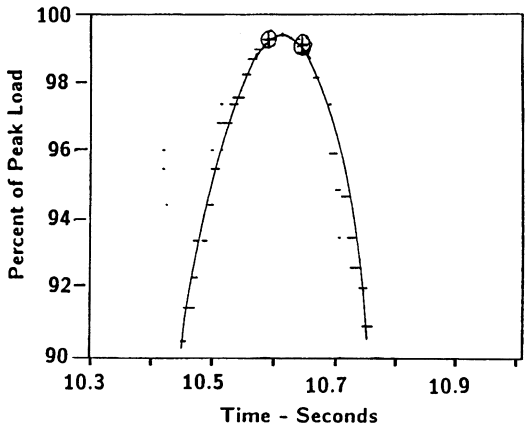

Figure 2. Load values as a function of time for he peak of a load cycle. Horizontal lines are multiple hits.

Figure 2 shows the assigned load of all hits allowed by the voltage gate on one cycle. The loads are plotted as a

function of test time. The two located events on this cycle are given as circled crosses. The approximate load curve is shown as a solid line. It is apparent that the assigned loads were close to the actual loads, but both the quantization errors and some scatter are present. Both located events occur very close to the peak load as was expected.

SUMMARY OF TEST PROCEDURE

The test proceeded in four stages. In the first stage, three and a half minutes of data was taken to determine the initial data rate. Well over an hour of running time was then used in getting the voltage-controlled gate set. The second stage was to be the start of the main run. This proceeded for an hour and eighteen minutes, at which time it was stopped because of problems with the loading equipment. The third stage was started the next morning and was continued for 23 hours. It was stopped because the blade surface in one of the oil can regions appeared to be disintegrating and loud noises were occurring on every cycle. The fourth stage was started several weeks later. This test lasted for a total of 36 minutes of running time with several stops to examine the blade. The upper skin in the suspect oil can region buckled and pulled away from the front spar. The loading was stopped and a tear in the skin along the edge of the spar was examined. Loading was restarted and continued for another six minutes when the skin buckled and tore perpendicular to the spar with apparent damage to the spar. This ended the test.

DATA ANALYSIS

In the analysis of this data, several terms describing the acoustic emission will be used. An event is the localized damage occurring in the blade which produces the acoustic pulse or burst. A hit is defined when the acoustic burst arrives at and is detected by a sensor. One event usually produces hits on several sensors. An event is defined by the software when all sensors of a triangle or rectangle are hit within the time it takes an acoustic signal to travel the longest distance between two sensors on the polygon. This time is defined by the acoustic velocity which was roughly measured at 3. 6 mm per microsecond. Some anisotropy was seen in the velocity and there is always some uncertainty as to which cycle of the acoustic signal was detected first. Therefore this time is increased by about 20% so as to include as many real events as possible. Inconsistent data sets (sets with wrong sensors or relative arrival times which did not correspond to an event located on the surface) were rejected in the Sandia location calculation. The definition of an event for the root region was that all three sensors at the comers of a triangle are hit within a 400 microsecond span and for the blade, all four sensors at the comers of a rectangle must be hit within a time span of 350 microseconds. To be kept as a located event, the calculated location must lie no more than 10% outside of the boundaries of the triangle or rectangle. The Spartan AT location algorithm used a similar logic for event definition but did not restrict the location to within the polygon defined by the hit sensors.

Post test analysis of the data was performed by a location program written at Sandia. This program directly read the binary Spartan AT data files. To calculate the location, the program used a non-linear least squares routine. For the blade array, an over determined data set was used which included the arrival times from all four corner sensors of the rectangle. While locations could be calculated from only the first three sensors hit, this approach produced a very large number of located events. Restricting the definition of an event to four sensors hit, insured that the event would have a large amplitude and relatively low signal distortion. Experience by many practitioners[3] suggests that such an event is more likely to be caused by fiber breakage than lower amplitude sources such as matrix crazing or rupture of the fiber matrix bond. One more criteria was applied to the calculated locations. Since the data was an over determined set, any errors in the time measurements would result in a less than perfect fit of the calculated location to the data. The non-linear least squares fitting program calculates a parameter which is an indication of the goodness of the fit. Any data set which did not produce a reasonable value of this parameter was discarded. The rejection criteria was determined after extensive experimentation with the program on a variety of data sets. There were more than sufficient data points remaining to show just where the damage was located. At most, discarding these points would give an underestimate of the intensity of the damage. With the magnitude of the damage that was occurring in this blade, a small fraction of the total number of emissions is more than capable of defining the damaged regions.

Examination of the raw data showed many sets from individual sensors which had signal rise times of only a few microseconds (for this system, the signal rise time is defined as the time between the first detection of the signal and the time of occurrence of the peak amplitude). The frequency dependent attenuation of fiberglass is such that only very large events will have frequency components above 100 KHz. Typical acoustic emission signals which have propagated from growing flaws will take several cycles of their dominant frequency to reach their peak amplitude. One cycle of a 50 KHz wave lasts 20 microseconds. Therefore, all signals with rise times less than 20 microseconds were declared invalid for source location. This does not mean

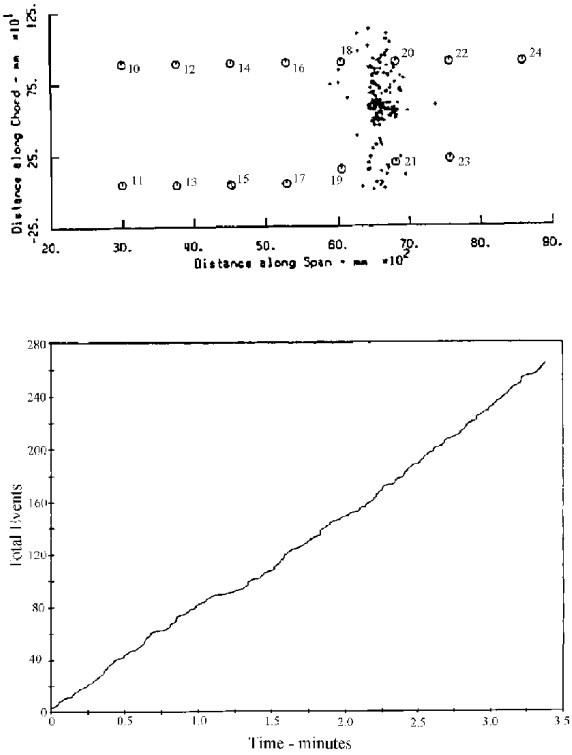

Figure 3. Event Locations and events as a function of time for Stage 1

that the signals were not real acoustic emission. What usually happens is that the system rearms itself to take new data in the middle of a signal and immediately triggers so that the signal actually started before the start time assigned it by the system. Thus such a signal, while produced by real damage, is useless in determining the location of the signal source.

TEST RESULTS, STAGE 1

The acoustic emission system was set up and run for about 3. 4 minutes without the voltage controlled gate. The data set was filtered to remove all sources which appeared to occur at times other than at the peak load. Figure 3 shows the location of these sources and the sum of the number of located sources as a function of time. There were about 260 located events in 150 cycles. Thus there was at least one event in every cycle in the 18,19,21,20 rectangle. The damage appears to have started at the first cycle which reached full load. The other oil can region, which occurred in the rectangle 12,13,15,14 showed no sign of locatable emission during this short run. No located emissions were seen in the root area covered by sensors I through 9.

The steady occurrence of locatable emission at the peak load of almost every cycle, as shown in Figure 3, strongly indicates that the peak test load exceeded the strength of this blade design in the region of rectangle 18,19,21,20.

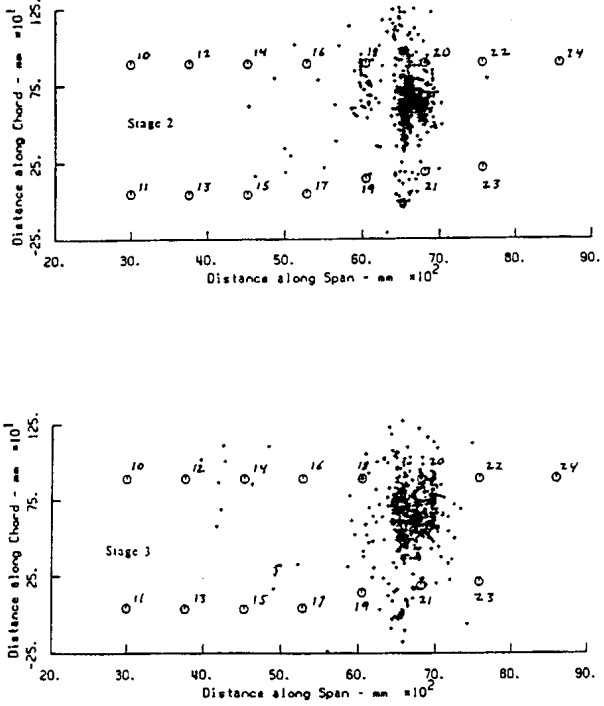

Figure 4. Event locations for Stage 2 and Stage 3

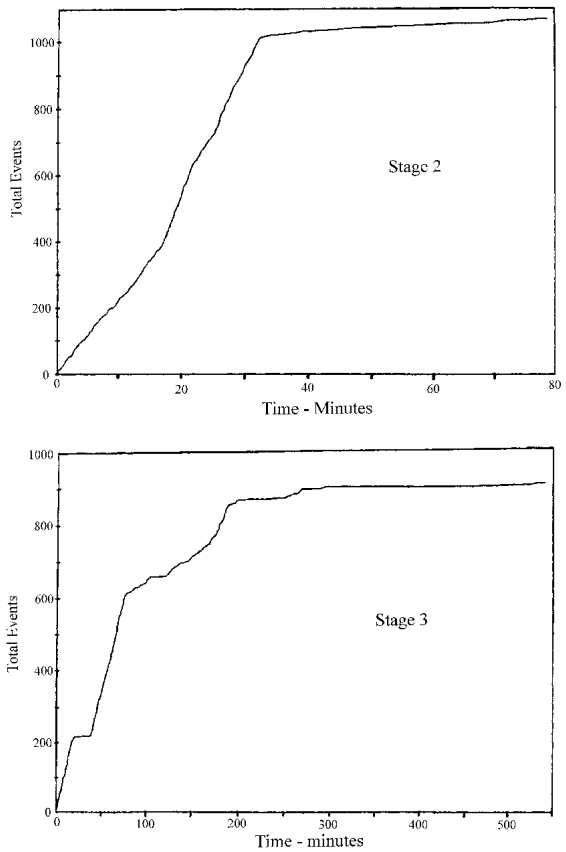

Figure 5. Events as a function of time for Stage 2 and Stage 3

TEST RESULTS, STAGE 2 AND 3

In stage 2, the test was started for a prolonged run. The voltage controlled gate was operational and data was taken when the load was above 8500 lbs. An hour and 18 minutes into the test, equipment problems occurred and loading was stopped. The next morning, stage 3 was started and ran for 23 hours. It was stopped because visual indication of damage in the skin was seen in rectangle 18,19,21,20. In addition, loud audible noises were heard on every cycle. There was also a decrease in blade stiffness.

Figure 4 shows the located emissions in stages 2 and 3 . Again most of the emissions appear to come from the oil can distortions in rectangle 18,19,21,20. Figure 5 shows the sum of the located sources as a function of time. Thirty-two minutes into the stage 2, there was an order of magnitude decrease in the rate of locatable emissions. A similar behavior is seen in stage 3 (the step between 20 and 28 minutes occurred when the loading was temporarily stopped) Notice that the temporary halt in loading did not change the event rate. The event rate did decrease at 78 minutes. A lower rate then continued, with some fluctuations, to 268 minutes. The rate again declined and ceased entirely at 549 minutes. The overall acoustic emission rate from the blade remained constant for the 23 hours of stage 3 but no events occurred where the acoustic burst excited sensors at all four corners of a rectangle within a 350 microsecond window for the last 14 hours of this stage.

Another way to examine the acoustic emission data is to plot hits from each sensor individually. Figure 6 shows totalized plots of the "energy" (actually the signal strength for each emission burst) as a function of time for sensors on top of the spar. Note that there are no significant changes in slope in any of these curves at 78 minutes (4680 seconds), 268 minutes (16,000 seconds) or 549 minutes (33,000 seconds). Thus the rates of located events have no correlation with acoustic emission rates seen at the individual sensors. Also notice that there was an increase in the "energy" rate around 72000 seconds (20 hours) for all sensors except 20. Closer examination showed that except for sensors 20, 21 and 24,7 there was an increase in the average "energy" per burst after 20 hours. Sensors 20 and 21 are located near the region where maximum damage occurred. There was very little sound material left in the skin in rectangle 18,19,21,20 by this point in the test. It is probable that this region weakened, transferring more load to the surrounding regions. This should increase the damage and lead to more acoustic energy being produced in each burst. Sensor 24 is a different case. Here the separation from sensor 22 (60 inches) is far enough so that the attenuation would allow few, if any,

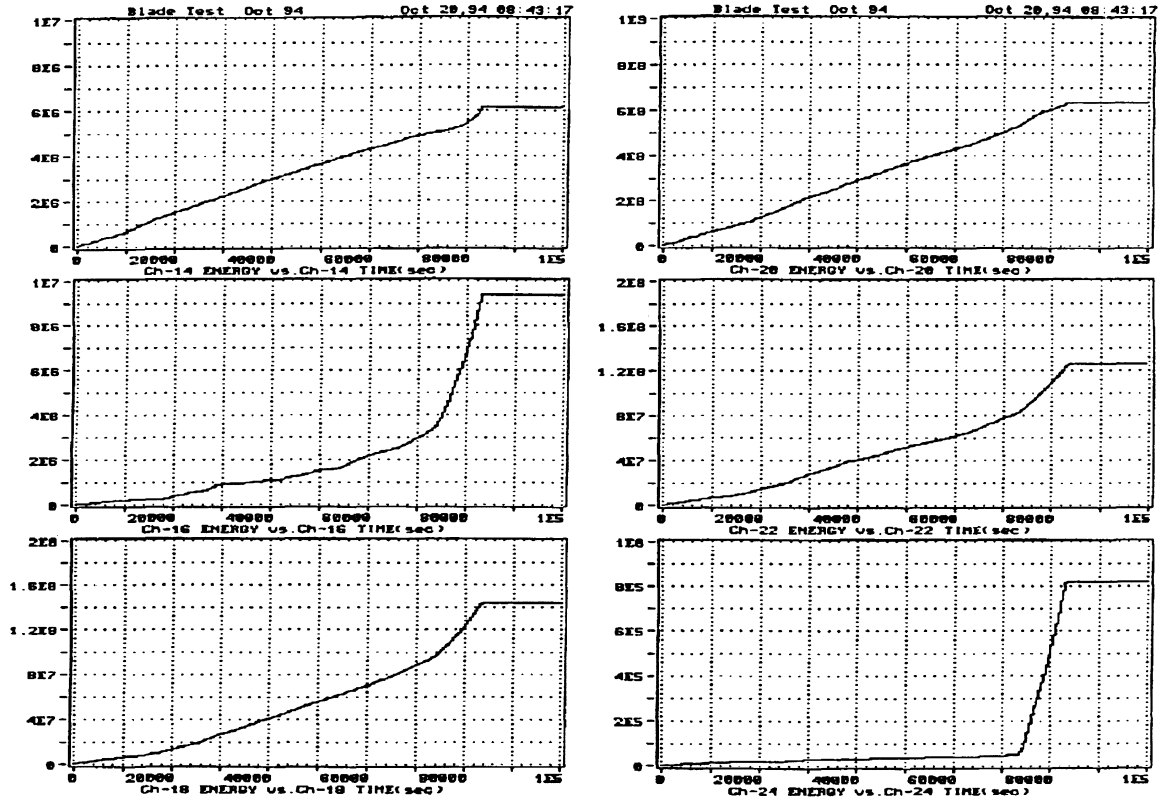

Figure 6. Total "energy" as a function of time for the leading edge sensors

signals to excite both sensors. The increase here was much larger, proportionally, than that seen in other sensors. The sensor was positioned to tiy to detect any damage occurring near the loading point on the blade and such damage is probably what is being seen. The average "energy" per burst decreased for sensor 24 beyond the 20 hour point which reinforces the assumption that this is a different mechanism from that seen in the other sensors.

were orders of magnitude less than those of sensors 18 through 21. There was also no indication of acoustic signals being introduced into the blade from the mounting block.

The location data from all four stages was combined. Figure 8 shows this data plotted in the critical rectangle 18,19,23,22. The symbols on the plot indicate the number of located events per square inch. The highest density is right in the middle of the region

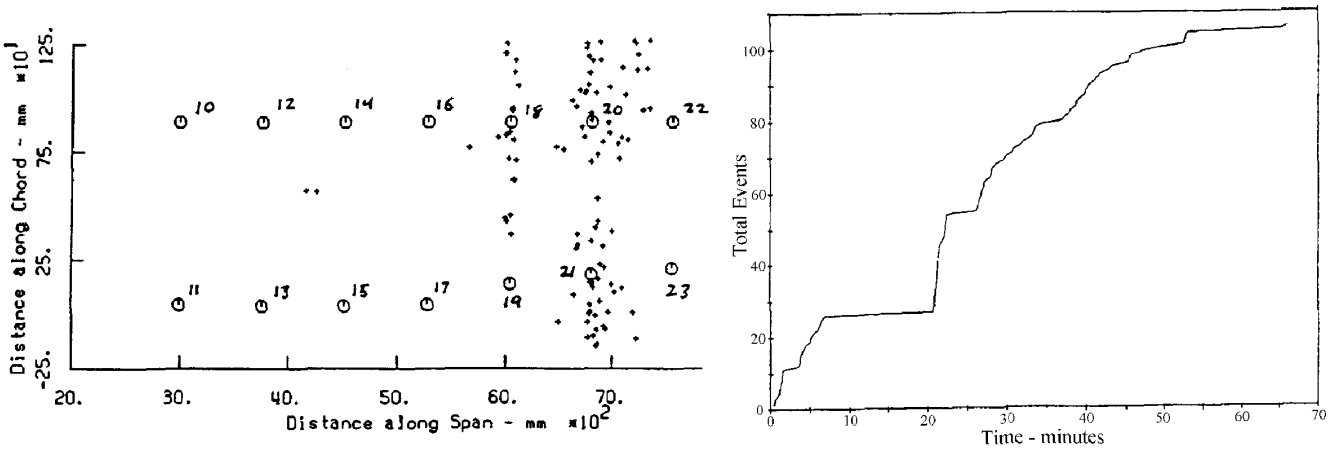

Figure 7. Event Locations and Events as a function of time for Stage 4

TEST RESULTS, STAGE 4

Stage 4 covered less than an hour of testing time. There were several halts during the test. The test was terminated at 66 minutes when the blade failed. A halt at 53 minutes was taken just after the skin ripped and separated from the top of the front spar. The test was restarted at 64 minutes and lasted about two minutes when the top skin buckled and ripped from the front spar toward the rear spar. Sensor 20 was just about over the rip and the failure broke the silicone rubber bond and launched sensor 20 skyward.

Figure 7 shows the map of located events for this stage and the located events as a function of time. There were not a large number of events located during this stage. The reason is not the lack of emission, but rather the gross damage in the skin which increased the acoustic attenuation, and the separation of the skin from the spar which interrupted the acoustic path to the rear sensors. These mechanisms prevented the acoustic bursts generated by even very energetic events from triggering all four sensors in a rectangle.

DISCUSSION

There was no indication of any damage occurring in the root region of the blade. The few located emissions were mapped at random over the surface. The totals of the signal strengths from sensors 2 through 9 showing oil can deformation. Visual observation of this area before the stage 4 run indicated expensive damage. The final failure of the blade also occurred very close to the area of maximum density of located events.

One should note that the highest density of located events is not along the line between sensor 18 and 20 where the initial tear in the skin took place. The tear effectively prevented any acoustic signals from being transmitted to sensors 19 and 21 and thus prevented location of this failure. For this reason, other types of acoustic emission analysis are often used in composite structures. Figure 6 shows the total signal strength ("energy") as a function of time for stage 3. Table I shows the total signal strength for several sensors from stage 3.

Sensor	Signal Strength	Sensor	Signal Strength
17	1.4 x 10^7	16	$9.4x10^6$
19	1.1 x 10^8	18	$1.4x10^8$
21	$6.7x10^8$	20	$6.4x10^8$
23	$5.5x10^7$	22	$1.3x10^8$

Table I. Total Signal Strength for Several Sensors in Stage 3 (arbitrary units)

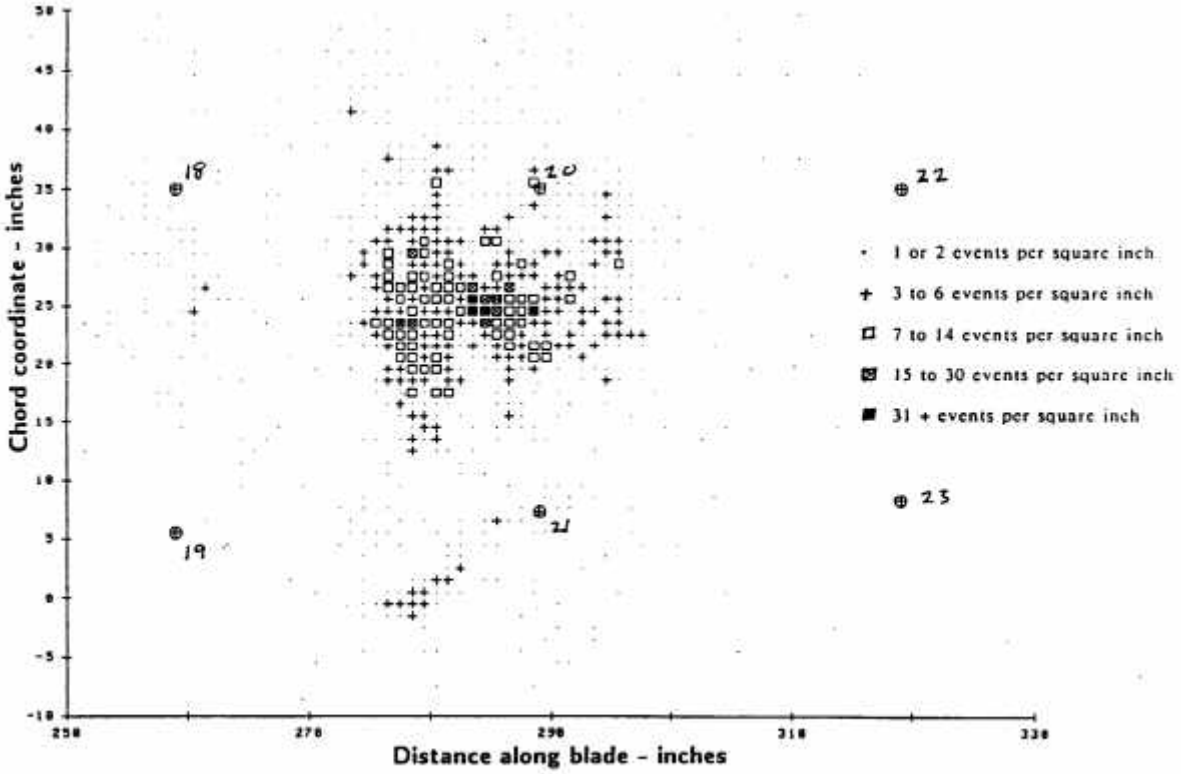

Figure 8. Density of located events for the entire test

From this table one can see that the center of the damaged area is between sensors 20 and 21 and part way back toward sensors 18 and 19. This corresponds very well with Figure 8.

Another way to look for damage is to look at the peak amplitude distributions for different sensors. For a given sensor and material, a higher peak amplitude usually indicates greater damage. (Note that the peak amplitude is measured on a logarithmic scale such that 20 dB corresponds to one order of magnitude). Figure 9 shows the peak amplitude distributions from sensors 13, 17 and 19 for stages 2, 3 and 4. The top graph is stage 2, the middle, stage 3, and the bottom is stage 4. For Stage I, except for sensor 21, there was essentially no emission with peak amplitudes at or above 80 dB. In stage 3, all sensors but 13 have shown a few hits above 80 dB but they are still in a distinct minority. In stage 4, there are far fewer hits on each sensor but some of the distributions have changed. Sensor 19 now has a distinct peak around 90 dB while 17 is still lacking any signals above 80 dB. This agrees with all of the previous data which indicates failure between sensors 19 and 21. However, we now see peaks with amplitudes above 80 dB for sensor 13. These peaks were not seen in data from sensors II, 17 nor from sensors 10, 12, 14, and 16. There are few located emissions near the rear spar in this region. The most plausible explanation for this data is that new damage occurred during stage 4 behind the rear spar between sensors 13 and 15. The damaged region would be far enough behind the spar that the attenuation prevents the detection of the signals at sensors 12 and 14.

CONCLUSIONS

This experiment shows that fatigue tests of large FRP wind turbine blades can be monitored by acoustic emission techniques and that the monitoring can produce useful information. The system showed that the peak load was too high so that it could have been decreased before significant damage was done to the blade. The data also showed that oil can deformation is not, of itself, detrimental to an FRP structure. The blade data indicated that the increase of the load exceeded the low cycle fatigue strength of the blade. The skin in the rectangle formed by sensors 18,19,21,20 went into oil can deformation, accompanied by degradation of the fiberglass skin. The rest of the blade did not appear to be damaged by this load. The skin in the rectangle formed by sensors 12,13,15,14 showed oil can deformation throughout this test but gave no significant acoustic emission and showed no sign of fiberglass degradation. In stage 4, there were small indications of another region of failure toward the trailing edge of the blade between sensors 13 and 15

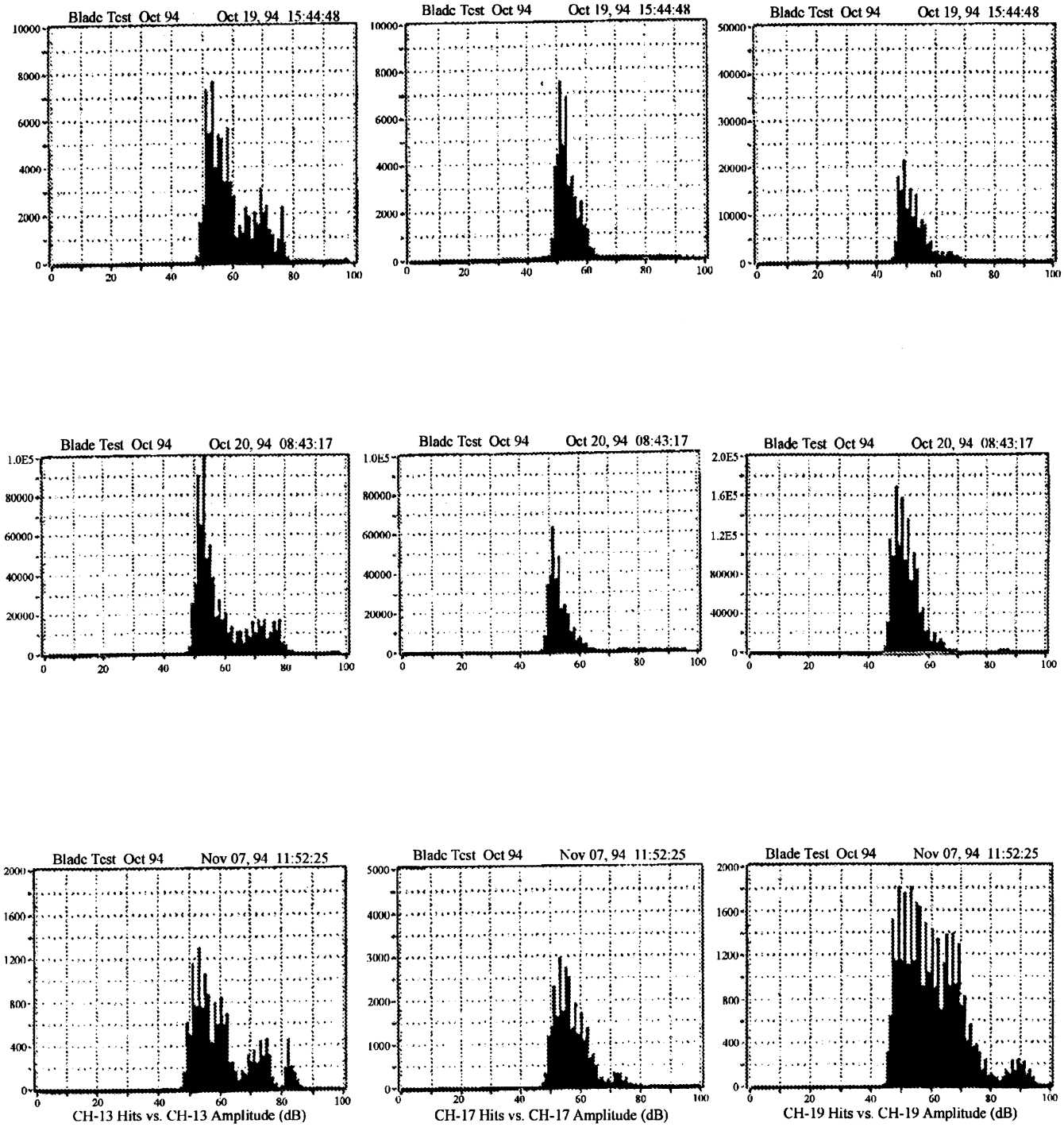

Figure 9. Peak amplitude distributions from Stages 2 (top), 3 (middle) and 4 (bottom) for sensors 13, 17 and 19

ACKNOWLEDGEMENT

The author would like to thank Jim Johnson, Mike Jenks and all the personnel of the NREL wind turbine testing facility for their valuable help and consultation. He would also like to thank Herb Sutherland of Sandia and Walt Musial of NREL for a critical review of this Paper.

REFERENCES

1. H. Sutherland, A. Beattie, B. Hansche, W. Musial, J. Allread, J. Johnson and M. Summers (1994), "The Application of Non-destructive Techniques to the Testing of a Wind Turbine Blade", Sandia National Laboratories Report SAND93-1380

2. A. G. Beattie (1983), "Acoustic Emission, Principals and Instrumentation", *Journal of Acoustic Emission*, 2(l-2):95-128

3. ASNT (1987), Nondestructive Testing Handbook, Volume 5, Acoustic Emission Testing, R. K. Miller and PMcIntireed. ASNT

4. J. Wei and J. McCarty (1993), "Acoustic Emission Evaluation of Composite Wind Turbine Blades During Fatigue Testing", *Wind Engineering* 17(6):266-274